

Formation and Decay Dynamics of Vitamin E Radical in the Antioxidant Reaction of Vitamin E

Kazuo Mukai,^{*1} Aya Ouchi,^{*1} Akiko Mitarai,¹ Keishi Ohara,¹ and Chihiro Matsuoka²

¹Department of Chemistry, Faculty of Science, Ehime University, Matsuyama 790-8577

²Department of Physics, Faculty of Science, Ehime University, Matsuyama 790-8577

Received October 27, 2008; E-mail: mukai@chem.sci.ehime-u.ac.jp

In order to understand the dynamics of antioxidant actions of vitamin E (α -, β -, γ -, and δ -tocopherols, TocH) in biological systems, kinetic study of the formation and decay reactions of vitamin E radicals (α -, β -, γ -, and δ -tocopheroxyls, Toc•) has been performed in organic solvents, using stopped-flow spectrophotometry. By mixing α -, β -, γ -, and δ -TocH with aryloxy radical (ArO•) in ethanol, the peaks of the UV-vis absorption due to α -, β -, γ -, and δ -Toc• radical appeared rapidly at ca. 430–340 nm, showed maxima, and then decayed gradually. The second-order rate constants (k_f and $2k_d$) for the formation and decay (that is, bimolecular disproportionation) reactions of α -Toc• were determined by comparing the observed curves with the simulation ones obtained by the numerical calculation of differential equations related to the above reactions. From the results, the wavelengths of absorption maxima (λ_{\max}^i) and molar extinction coefficients (ε_i) ($i = 1-4$) of the optical spectra were determined for α -Toc• radical. Notable solvent effects have been observed for the reaction rates (k_f and $2k_d$) and absorption spectra (λ_{\max}^i and ε_i) of α -Toc• radical. The scheme of the formation and decay reactions of α -, β -, γ -, and δ -Toc• radicals has been discussed based on the results obtained.

Vitamin E (α -, β -, γ -, and δ -tocopherols, TocH) is well known to scavenge free radicals (LOO• and LO•) generated in biological systems. The antioxidant actions of the tocopherols have been ascribed to the hydrogen abstraction reaction from a phenolic hydroxy group, producing corresponding tocopheroxyl (Toc•) radicals (Figure 1 and reaction 1).¹⁻⁴ The Toc• radicals produced may combine with another peroxy (LOO•) radical (reaction 2).¹ If tocopherols exist in biomembranes and oils, the Toc• radicals may react with unsaturated lipids (LH) (reaction 3) and lipid hydroperoxides (LOOH) (reaction 4).⁵⁻⁹ These reactions 3 and 4 are known as prooxidant reactions, which induce the degradation of unsaturated lipids. Toc• radicals may be regenerated to TocH by vitamin C (ascorbate anion, AsH⁻) (reaction 5)^{2,3,10,11} and/or ubiquinol¹² in biological systems, to protect the above prooxidant effects. Further, Toc• radicals disappear by bimolecular reaction with another Toc• to give non-radical products (NRP) (reaction 6).^{1,13-19}



As described above, α -, β -, γ -, and δ -Toc• radicals are important key radicals, which appear in the process of the antioxidant and prooxidant actions of α -, β -, γ -, and δ -TocH.

Detailed kinetic studies have been performed for reactions 1 and 5, and the mechanism involved has been studied extensively by several investigators.^{1-4,11,20-22} However, examples of the measurement of the rate constants (k_2 , k_3 , k_4 , and

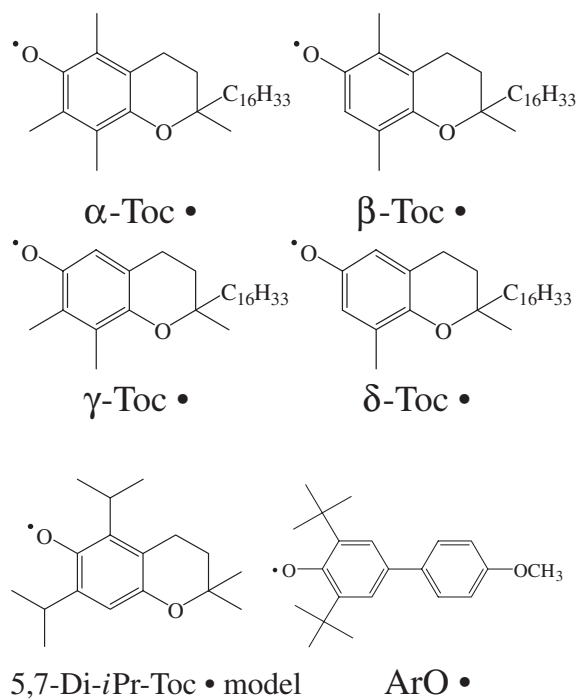


Figure 1. Molecular structures of α -, β -, γ -, and δ -tocopheroxyl (Toc•), 5,7-diisopropyltocopheroxyl model (5,7-Di-*i*-Pr-Toc•), and aryloxy (ArO•) radical.

$2k_d$) for reactions 2, 3, 4, and 6 are limited, because of the instability of α -, β -, γ -, and δ -Toc \bullet radicals. The reaction of LOO \bullet with α -Toc \bullet radical (reaction 2) is very fast with a rate constant of $3 \times 10^8 \text{ M}^{-1} \text{ s}^{-1}$.²³ The reaction rates (k_3 and k_4) have been measured by using more stable 5,7-diisopropyl-tocopheroxyl (5,7-Di-*i*-Pr-Toc \bullet) radical (Figure 1), and the structure–activity relationship has been clarified for reactions 3 and 4.^{7,24,25}

In previous work,²⁶ we measured the reaction rates (k_s) of α -, β -, γ -, and δ -tocopherols with 2,6-di-*t*-butyl-4-(4-methoxyphenyl)phenoxy (ArO \bullet) (abbreviated to aryloxy, hereafter) (Figure 1) in ethanol (reaction 7) using stopped-flow spectrophotometry. ArO \bullet can be regarded as a model for active oxygen radicals (LOO \bullet and others) in biological systems.



The second-order rate constants (k_s) obtained were 5.12×10^3 (α -TocH), 2.24×10^3 (β -TocH), 2.42×10^3 (γ -TocH), and 1.00×10^3 (δ -TocH) $\text{M}^{-1} \text{ s}^{-1}$ in ethanol at 25.0 °C. ArO \bullet -scavenging rates (k_s) increased with increasing the number of methyl substituents at the phenol ring, that is, the electron-donating capacity of tocopherols. The relative rates ($\alpha:\beta:\gamma:\delta = 100:44:47:20$) agreed well with those obtained in studies on the reactivity (k_{inh}) of TocH toward poly(peroxy-styryl)peroxy radicals (100:41:44:14) in chlorobenzene using the O₂ consumption method (reaction 1).¹ The results suggest that the relative reactivity of TocH in solution probably does not depend on the type of oxyradicals (ArO \bullet and LOO \bullet) used.^{26–28}

In the present work, in order to understand the dynamics of antioxidant actions of vitamin E (α -, β -, γ -, and δ -tocopherols, TocH) in biological systems, kinetic study of formation and decay reactions 7 and 6 of vitamin E radicals (α -, β -, γ -, and δ -Toc \bullet) has been performed in several organic solvents, using stopped-flow spectrophotometry. By mixing α -, β -, γ -, and δ -TocH with ArO \bullet in organic solvents, UV–vis absorption spectra due to Toc \bullet radicals appeared rapidly in the wavelength region of 340–430 nm, showed a maximum, and then decayed gradually. The simulation of the formation and decay curve of α -Toc \bullet was performed by the numerical calculation of differential equations derived from reactions 6 and 7, using the fourth-order Runge–Kutta method.²⁹ From the results, the rate constant ($2k_d$) for the decay reaction and the molar extinction coefficients (ϵ) of the UV–vis absorption spectra of α -Toc \bullet radical were determined.

Experimental

α -, β -, γ -, and δ -Tocopherols used in the present work were kindly supplied by Eisai Co., Ltd. ArO \bullet radical was prepared according to the method of Rieker and Scheffler.³⁰

The kinetic data were obtained with a Unisoku Model RSP-1000 stopped-flow spectrophotometer by mixing equal volumes of solutions of antioxidants and ArO \bullet under nitrogen atmosphere.²⁶ The shortest time for mixing two solutions and recording the first data point (that is, dead time) was 10–20 ms. The reaction was monitored with either single wavelength detection or photo-diode array detector attached to the stopped-flow spectrophotometer. All measurements were performed at 25.0 ± 0.5 °C.

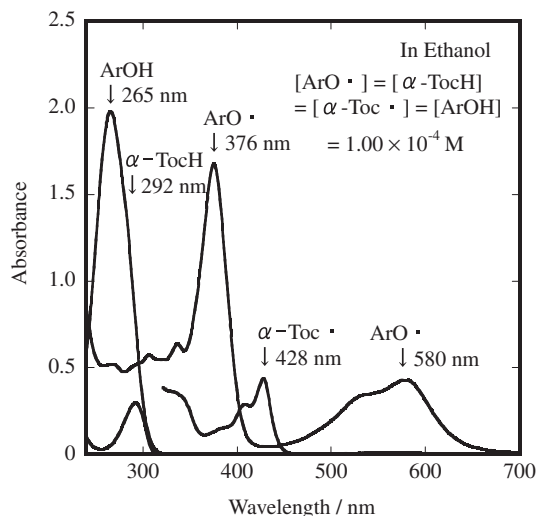


Figure 2. UV–visible absorption spectra of ArOH, α -TocH, ArO \bullet , and α -Toc \bullet with the same concentrations of $1.00 \times 10^{-4} \text{ M}$ in ethanol.

Results

UV–Vis Absorption Spectra of α -, β -, γ -, and δ -Tocopheroxyl Radicals. The aryloxy radical (ArO \bullet) is stable in the absence of α -tocopherol, and shows absorption peaks at $\lambda_{\text{max}} = 376 \text{ nm}$ ($\epsilon = 16900 \text{ M}^{-1} \text{ cm}^{-1}$; $1 \text{ M} = 1 \text{ mol dm}^{-3}$), 580 nm ($\epsilon = 4330 \text{ M}^{-1} \text{ cm}^{-1}$), and 530 nm (shoulder) ($\epsilon = 3100 \text{ M}^{-1} \text{ cm}^{-1}$) in ethanol solution. The phenol precursor (ArOH) of ArO \bullet and α -tocopherol show absorption peaks at $\lambda_{\text{max}} = 265 \text{ nm}$ ($\epsilon = 19800 \text{ M}^{-1} \text{ cm}^{-1}$) and 292 nm ($\epsilon = 2990 \text{ M}^{-1} \text{ cm}^{-1}$), respectively, in ethanol; no absorptions were observed in the visible absorption region, as shown in Figure 2. By adding the ethanol solution of α -tocopherol ($1.88 \times 10^{-3} \text{ M}$) to the solution of ArO \bullet ($3.33 \times 10^{-5} \text{ M}$) (1:1 in volume) at 25.0 °C, the absorption spectrum of ArO \bullet disappeared quickly, and changed to that of α -tocopheroxyl with four absorption peaks at $\lambda_{\text{max}} = 428, 408, 387\text{sh}$, and $340\text{sh} \text{ nm}$ (Figure 3a). α -Tocopheroxyl is unstable at 25.0 °C, and its absorption peaks decrease gradually after passing through the maximum (Figure 4a). The spectrum of the α -Toc \bullet at $t_{\text{max}} = 504 \text{ ms}$ is shown in Figure 3a. The absorption spectra of ArOH, ArO \bullet , α -TocH, and α -Toc \bullet having the same concentration of $1.00 \times 10^{-4} \text{ M}$ are shown in Figure 2.

The reactions of α -TocH with ArO \bullet were also performed in dichloromethane, chloroform, diethyl ether, benzene, hexane, and heptane solvents. The formation and decay curves of α -Toc \bullet in benzene and the absorption spectrum at $t_{\text{max}} = 365 \text{ ms}$ are shown in Figures 4c and 3b, respectively. The values of λ_{max}^i and ϵ_i ($i = 1-4$) obtained for α -Toc \bullet radical are listed in Table 1. The values of ϵ_i were determined by the analyses of the formation and decay curves of the α -Toc \bullet radical, as described later.

Similarly, upon mixing of ArO \bullet ($6.84 \times 10^{-5} \text{ M}$) with excess β -TocH ($3.56 \times 10^{-3} \text{ M}$) in ethanol, two absorption peaks at 431 and 409 nm of β -Toc \bullet appeared instantly, showed a maximum, and then its intensity decreased gradually, as shown in Figure 5a and Figure 6. Differing from the case of

α -Toc•, the absorption spectrum of ArO• does not disappear completely by the reaction and weak absorption peaks remain at 376 and 580 nm, although the concentration of the ArO• ($[\text{ArO}\bullet]$) is less than 5% of the initial concentration of ArO• ($[\text{ArO}\bullet]_{t=0} = 6.84 \times 10^{-5} \text{ M}$).

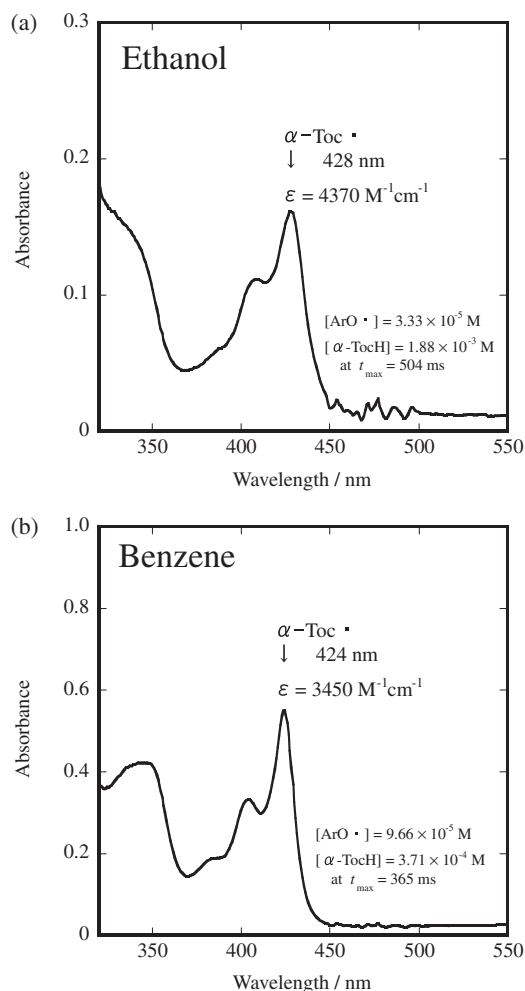


Figure 3. UV-vis absorption spectra of α -Toc• in (a) ethanol and (b) benzene at $t_{\text{max}} = 504$ and 365 ms, respectively.

By reacting γ -TocH ($4.81 \times 10^{-3} \text{ M}$) with ArO• ($6.97 \times 10^{-5} \text{ M}$) in ethanol, the absorption spectrum of γ -Toc• was observed at $\lambda_{\text{max}} = 432 \text{ nm}$. The absorption spectrum at $t_{\text{max}} = 200 \text{ ms}$ is shown in Figure 5b. The concentration of ArO• remaining at $t_{\text{max}} = 200 \text{ ms}$ was estimated to be $1.4 \times 10^{-5} \text{ M}$, which corresponds to about 20% of the initial concentration of ArO• ($[\text{ArO}\bullet]_{t=0}$). The result indicates the existence of equilibrium in reaction 7. As shown in Figure 2, the absorption spectrum of ArO• shows a minimum at 420–440 nm ($\epsilon = 200 \text{ M}^{-1} \text{ cm}^{-1}$). Therefore, the absorbance of the ArO• at 432 nm is very weak, and is almost negligible compared with that of the γ -Toc•. Similarly, weak absorption spectrum of δ -Toc• was observed at 432 nm, and decreased rapidly with time, as shown in Figure 5c and Figure 6, respectively.

As shown in Figure 6, the same concentration of ArO• ($8.88 \times 10^{-5} \text{ M}$) was used for the reaction with α -, β -, γ -, and δ -tocopherols. Therefore, we can expect that the absorption intensities of β -, γ -, and δ -Toc• at t_{max} are similar to that of α -Toc•, if the values of the molar extinction coefficient (ϵ) of β -, γ -, and δ -Toc• are similar to that of α -Toc•. However, the intensities of Toc• radicals at t_{max} decreased rapidly in the order of α -Toc• (Absorbance = 0.408 at $\lambda_{\text{max}} = 428 \text{ nm}$) > β -Toc• (0.131 at 431 nm) > γ -Toc• (0.073 at 432 nm) > δ -Toc• (0.034 at 434 nm) in ethanol, as shown in Figure 6. The reason will be discussed in a later section.

The Rates of the Aryloxy-Radical-Scavenging (k_s) of α -, β -, γ -, and δ -Tocopherols in Organic Solvents. Measurements of the rate constant (k_s) for the reaction of ArO• radical with α -, β -, γ -, and δ -TocH were performed in ethanol solution (reaction 7). The decay rate of ArO• radical was measured by following the decrease in absorbance at 376 and/or 580 nm of the ArO•.²⁶ The pseudo-first-order rate constants (k_{obsd}) at 376 and/or 580 nm were linearly dependent on the concentration of TocH ($[\text{TocH}]$), and thus the rate equation is expressed as

$$-d[\text{ArO}\bullet]/dt = k_{\text{obsd}}[\text{ArO}\bullet] = k_s[\text{TocH}][\text{ArO}\bullet] \quad (8)$$

where k_s is the second-order rate constant for oxidation of TocH by ArO• radical. The rate constants (k_s) were obtained by plotting k_{obsd} against $[\text{TocH}]$. The rate constants (k_s) of α -, β -, γ -, and δ -TocH increase in the order of δ -TocH < γ -TocH \approx β -TocH < α -TocH, as described in Introduction.²⁶

Table 1. The Values of Dielectric Constant ($\epsilon_{\text{dielectric-constant}}$), UV-Visible Absorption Maxima (λ_{max}^i), and Molar Extinction Coefficients (ϵ_i) ($i = 1$ –4) of the α -Tocopheroxyl Radical in Several Organic Solvents

Solvent	$\epsilon_{\text{dielectric-constant}}$	$\lambda_{\text{max}}^1/\text{nm}^{\text{a}}$ ($\epsilon_1/\text{M}^{-1} \text{ cm}^{-1}$)	$\lambda_{\text{max}}^2/\text{nm}^{\text{a}}$ ($\epsilon_2/\text{M}^{-1} \text{ cm}^{-1}$)	$\lambda_{\text{max}}^3/\text{nm}^{\text{a}}$ ($\epsilon_3/\text{M}^{-1} \text{ cm}^{-1}$)	$\lambda_{\text{max}}^4/\text{nm}^{\text{a}}$ ($\epsilon_4/\text{M}^{-1} \text{ cm}^{-1}$)
Ethanol	24.58	428 (4370) 426 (3800) ^b	408 (3010)	387sh ^d (1630)	340sh ^d (3790)
Dichloromethane	8.931	427 (4100)	408 (2630)	387 (1150)	335 (3120)
Chloroform	4.806	427 (4320)	408 (2920)	387 (1320)	345 (3270)
Diethyl ether	4.335	421 (3500)	400 (2150)	381 (1270)	341 (2810)
Benzene	2.3	424 (3450) 423 (6700) ^c	404 (2070)	383sh ^d (1170)	344 (2620)
Heptane	1.924	418 (3080)	398 (1860)	374 (1360)	345 (2700)
Hexane	1.880	418 (2500)	398 (1520)	373 (1290)	341 (2040)

a) Experimental errors in λ_{max}^1 , λ_{max}^2 , and λ_{max}^3 are $\pm 1 \text{ nm}$, and in λ_{max}^4 are $\pm 5 \text{ nm}$. b) See Ref. 19. c) See Ref. 31. d) sh: Shoulder.

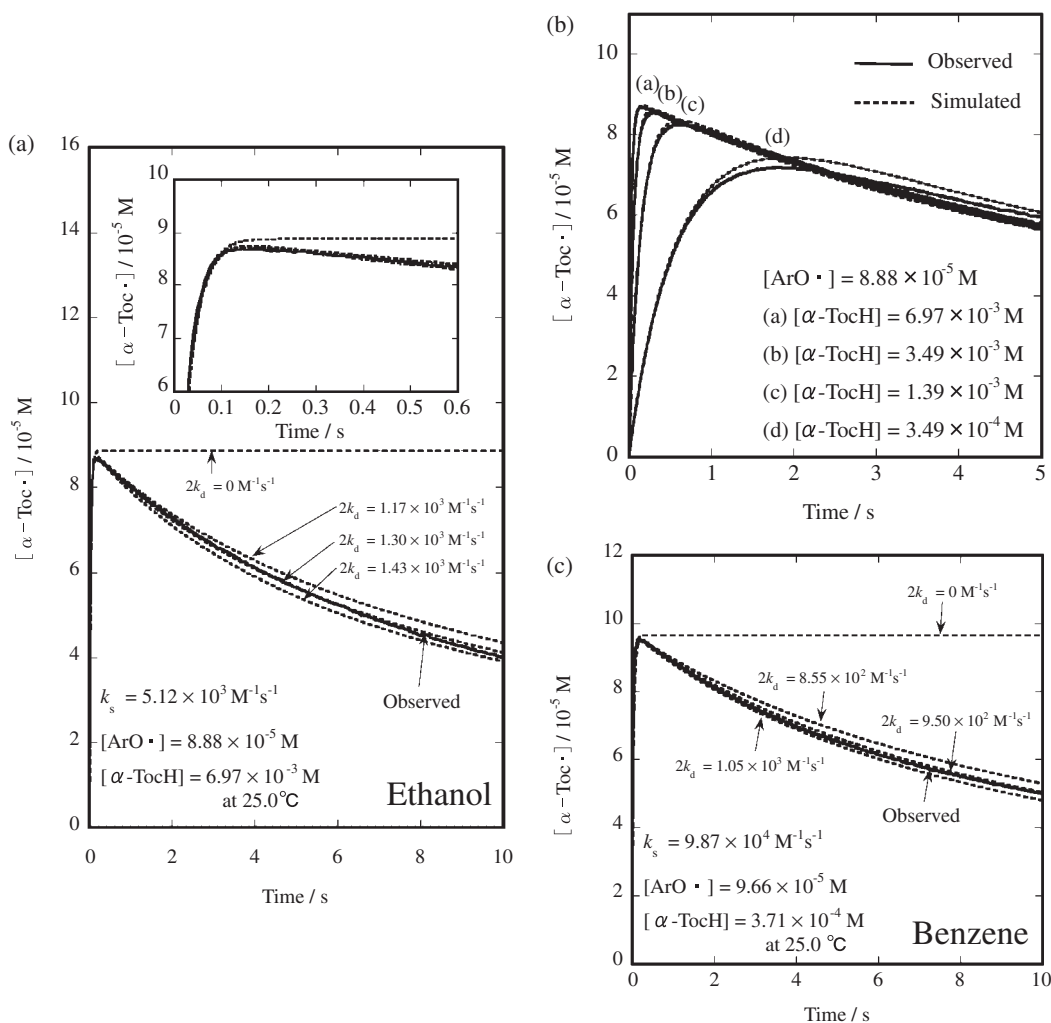
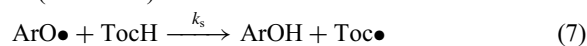


Figure 4. Time dependence of the concentrations of α -Toc \bullet radical observed at λ_{\max}^1 (Table 1) during reaction of ArO \bullet with α -TocH in (a) ethanol, (b) ethanol, and (c) benzene at 25.0 °C (Solid line). Dotted line is a simulation curve. The values of $[\text{ArO}\bullet]_{t=0}$ and $[\alpha\text{-TocH}]_{t=0}$ are shown in Figures 4a–4c.

In the case of α -TocH, the measurements were performed in several organic solvents. The reaction rates (k_s) increased with decreasing polarity of solvent (Table 2), as reported in previous work.³³ When the logarithm of the rate constant ($\log k_s$) was plotted as a function of the reciprocal of the solvent dielectric constants ($1/\epsilon_{\text{dielectric-constant}}$), a linear correlation was observed.³³

Analysis of the Formation and Decay Reactions of α -, β -, γ -, and δ -Tocopheroxyl Radicals in Organic Solvents, Using the Fourth-Order Runge–Kutta Method. By reacting α -TocH with ArO \bullet in organic solvents (reaction 7), α -Toc \bullet radical is produced rapidly, and disappears by a bimolecular reaction (reaction 6).^{1,13–19}



Where the rate of ArO \bullet -scavenging (k_s) in reaction 7 equals that of Toc \bullet -formation (k_f), that is, $k_s = k_f$. Reaction equations included in the above reactions 6 and 7 are as follows (eqs 9–13):

$$-d[\text{ArO}\bullet]/dt = k_s[\text{TocH}][\text{ArO}\bullet] \quad (9)$$

$$d[\text{ArOH}]/dt = k_s[\text{TocH}][\text{ArO}\bullet] \quad (10)$$

$$-d[\text{TocH}]/dt = k_s[\text{TocH}][\text{ArO}\bullet] \quad (11)$$

$$d[\text{Toc}\bullet]/dt = k_s[\text{TocH}][\text{ArO}\bullet] - 2k_d[\text{Toc}\bullet]^2 \quad (12)$$

$$d[\text{NRP}]/dt = 2k_d[\text{Toc}\bullet]^2 \quad (13)$$

There are three relations (eqs 14–16) between the concentrations of constituents.

$$[\text{ArO}\bullet]_t + [\text{ArOH}]_t = [\text{ArO}\bullet]_{t=0} = c_1 \quad (14)$$

$$[\text{TocH}]_t + [\text{Toc}\bullet]_t + 2[\text{NRP}]_t = [\text{TocH}]_{t=0} = c_2 \quad (15)$$

$$-[\text{ArO}\bullet]_t + [\text{TocH}]_t = -[\text{ArO}\bullet]_{t=0} + [\text{TocH}]_{t=0} = -c_1 + c_2 \quad (16)$$

Where, for instance, $c_1 = [\text{ArO}\bullet]_{t=0}$ is a concentration of ArO \bullet at $t=0$, and $[\text{ArO}\bullet]_t$ is a concentration of ArO \bullet at $t=t$. Therefore, only eqs 9, 12, and 13 are independent equations. Setting $[\text{ArO}\bullet]_t = X_1$, $[\text{Toc}\bullet]_t = X_2$, and $[\text{NRP}] = X_3$, we can obtain

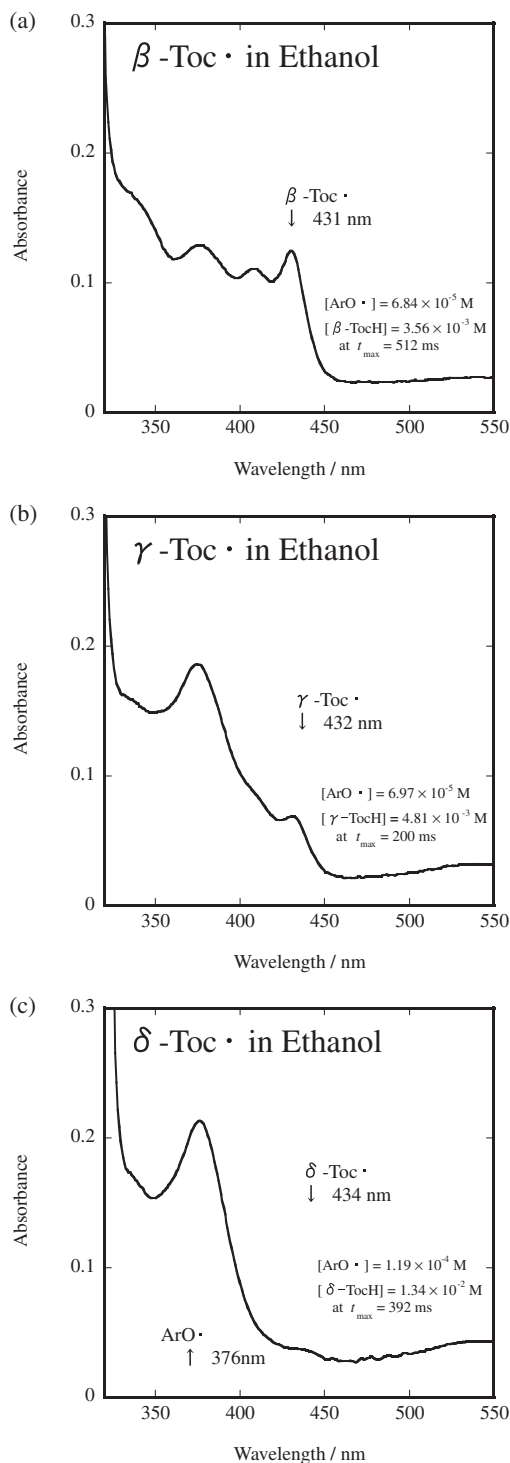


Figure 5. UV-vis absorption spectra of (a) β -Toc•, (b) γ -Toc•, and (c) δ -Toc• radicals in ethanol solution at $t_{\max} = 512, 200,$ and 392 ms, respectively.

$$-dX_1/dt = k_s(c_2 - X_2 - X_3)X_1 \quad (17)$$

$$dX_2/dt = k_s(c_2 - X_2 - X_3)X_1 - 2k_dX_2^2 \quad (18)$$

$$dX_3/dt = 2k_dX_2^2 \quad (19)$$

Equations 17, 18, and 19 were solved numerically using the fourth-order Runge-Kutta method, as performed by Lucarini et al.^{15,29}

The simulation of the formation and decay curves of α -Toc• at $\lambda_{\max}^1 = 428$ nm in ethanol was performed by varying the rate ($2k_d$) of bimolecular reaction and the molar extinction coefficient (ε_1), where the concentration of α -Toc• radical, $[\alpha\text{-Toc}\bullet]_t$, was calculated from the absorption spectra, by using Lambert-Beer's equation (Absorbance (A_t) = $\varepsilon_1[\alpha\text{-Toc}\bullet]_t$). The value of k_s ($=k_f = 5.12 \times 10^3 \text{ M}^{-1} \text{ s}^{-1}$)²⁶ in ethanol was used for the calculation. As shown in Figure 4b, the concentration (that is, the absorbance) of α -Toc• radical at t_{\max} increases with increasing the concentration of α -TocH and approaches a constant value, because at high concentration of α -TocH α -Toc• appears rapidly and the decay of α -Toc• due to bimolecular reaction is very small and negligible. Therefore, we can estimate the ε_1 value of α -Toc• radical, using the relation (Absorbance (of α -Toc• at t_{\max}) = $\varepsilon_1 \times [\text{ArO}\bullet]_{t=0}$). The results of the analysis performed for α -Toc• are shown in Figures 4a and 4b. For comparison, the simulation curve calculated for the case of $k_d = 0 \text{ M}^{-1} \text{ s}^{-1}$ is also shown in Figure 4a.

The good agreement between the observed and simulation curves was obtained for three different concentrations of α -TocH ($[\alpha\text{-TocH}] = 6.97 \times 10^{-3}, 3.49 \times 10^{-3},$ and $1.39 \times 10^{-3} \text{ M}$) at $t = 0-10$ s, if we use the values of k_s ($=5.12 \times 10^3 \text{ M}^{-1} \text{ s}^{-1}$), k_d ($=1.30 \times 10^3 \text{ M}^{-1} \text{ s}^{-1}$), and ε_1 ($=4370 \text{ M}^{-1} \text{ cm}^{-1}$ at $\lambda_{\max}^1 = 428$ nm) (Figure 4b). On the other hand, when the concentration of α -TocH is lower ($[\alpha\text{-TocH}] = 3.49 \times 10^{-4} \text{ M}$), the agreement was not sufficient at $t > 1$ s. If the concentration of α -TocH is low, the rate of $\text{ArO}\bullet$ -scavenging ($-d[\text{ArO}\bullet]/dt$) is slow, and thus the α -Toc• radical generated will react with the $\text{ArO}\bullet$ radical remaining in solution, inducing the decrease of the concentration of the α -Toc•. As shown in Figure 4a, the concentration of α -Toc• ($[\alpha\text{-Toc}\bullet]_t = 8.71 \times 10^{-5} \text{ M}$) at $t_{\max} = 145$ ms is similar to the initial concentration of $\text{ArO}\bullet$ ($[\text{ArO}\bullet]_{t=0} = 8.88 \times 10^{-5} \text{ M}$), if the concentration of α -TocH is high ($[\alpha\text{-TocH}] = 6.97 \times 10^{-3} \text{ M}$) and thus $\text{ArO}\bullet$ and α -Toc• rapidly disappear and appear, respectively.

The measurements of the formation and decay curves of α -Toc• radical were performed in several solvents. In dichloromethane, chloroform, and benzene, the good agreements between the observed and simulation curves were obtained at $t = 0-10$ s, indicating that the decay of α -Toc• radical is due to bimolecular reaction (Figure 4c). On the other hand, in diethyl ether, heptane, and hexane, notable disagreements were observed, if the analyses were performed by assuming a simple bimolecular reaction, as shown in Figure 7a. Details of the analyses of the decay reaction of α -Toc• in these solvents will be described in the Discussion.

Discussion

Optical Spectra (λ_{\max} and ε) of α -, β -, γ -, and δ -Tocopheroxyl Radicals in Organic Solvents. α -, β -, γ -, and δ -Toc• radicals play an important role in the antioxidant and prooxidant actions of tocopherols (reactions 1-6), as described in the Introduction. Therefore, the measurements of the ESR and ENDOR spectra of Toc• radicals were performed in toluene under vacuum, and the proton hyperfine coupling constants (hfcc) (a_i^{H}) were correctly determined.³⁴⁻³⁶

On the other hand, the measurements of the UV-vis absorption spectra are difficult, because α -, β -, γ -, and δ -Toc• radicals are unstable. We reported the UV-vis absorption spectrum of a stable 5,7-diisopropyltocopheroxyl radical model (Figure 1) in ethanol.³⁷ As listed in Table 3, the values of λ_{\max}^i and ε_i ($i = 1-4$) for α -Toc• in ethanol are similar to those of 5,7-diisopropyltocopheroxyl model radical, suggesting that the values of ε_i obtained are reasonable. Boguth and Niemann³¹ and Gregor et al.¹⁹ reported the absorption spectrum of α -Toc• obtained by the reaction of α -TocH with DPPH radical in benzene and ethanol solution, respectively. The values of λ_{\max}^1 (=423 nm in benzene and 426 nm in ethanol) are similar to those (424 and 428 nm), respectively, observed in the present work. However, the value of ε_1 ($6700 \text{ M}^{-1} \text{ cm}^{-1}$) in benzene is about twice as large as that ($3420 \text{ M}^{-1} \text{ cm}^{-1}$) obtained in the present work. On the other hand, the value ($3800 \text{ M}^{-1} \text{ cm}^{-1}$) in

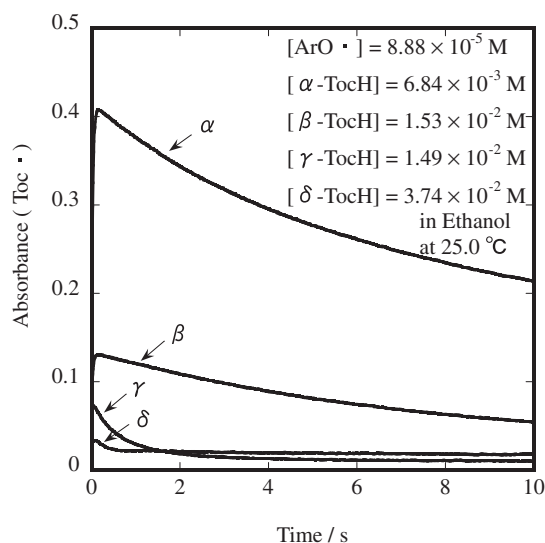


Figure 6. Time dependence of the absorbance of α -Toc• (at 428 nm), β -Toc• (at 431 nm), γ -Toc• (at 432 nm), and δ -Toc• (at 434 nm) radicals produced by the reaction of α -, β -, γ -, and δ -TocH with ArO• radical in ethanol at 25.0 °C, respectively. The values of $[\text{ArO}\cdot]_{t=0}$ and $[\text{TocH}]_{t=0}$ are shown in Figure 6.

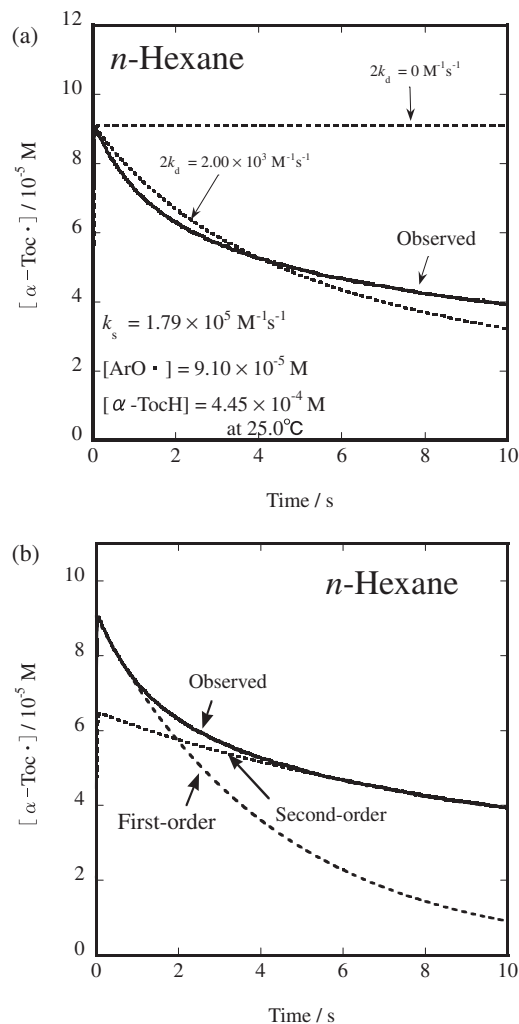


Figure 7. Time dependence of the concentrations of α -Toc• radical observed at 418 nm during reaction of ArO• with α -TocH in hexane at 25.0 °C (Solid line). Dotted lines are simulation curves calculated (a) by assuming a bimolecular reaction and (b) by assuming first-order and second-order decays (see text). The values of $[\text{ArO}\cdot]_{t=0}$ and $[\alpha\text{-TocH}]_{t=0}$ are shown in Figure 7a.

Table 2. Second-Order Rate Constants for the Aryloxy-Radical-Scavenging (k_s) of α -Tocopherol and for the Bimolecular Reaction ($2k_d$) of α -Tocopheroxyl Radical and Equilibrium Constant (K_{21}) at 25.0 °C in Organic Solvents

Solvent	$k_s/\text{M}^{-1} \text{ s}^{-1}$ ^{a)}	$2k_d/\text{M}^{-1} \text{ s}^{-1}$ ^{b)} (Present work)	$K_{21} = k_{-21}/k_{21}$ /M	$2k_d/\text{M}^{-1} \text{ s}^{-1}$ (Previous work)
Ethanol	5.12×10^3	1.30×10^3	$>10^{-3}$	1.03×10^3 , ^{c)} 1.4×10^3 , ^{d)} 1.06×10^3 ^{e)}
CH_2Cl_2	3.25×10^4	3.00×10^2	$>10^{-3}$	—
CHCl_3	2.76×10^4	3.00×10^4	$>10^{-3}$	1.9×10^2 ^{f)}
Diethyl ether	1.47×10^4	1.70×10^3	5.9×10^{-4}	—
Benzene	9.87×10^4	9.50×10^2	$>10^{-3}$	8.8×10^2 , ^{f)} 3×10^3 , ^{g)} 1.1×10^3 , ^{h)} 6.03×10^3 ⁱ⁾
Heptane	2.02×10^5	1.70×10^3	8.6×10^{-4}	—
Hexane	1.79×10^5	1.00×10^3	9.2×10^{-4}	3.12×10^3 ^{e)}

a) Experimental errors are $\pm 5\%$. b) Experimental errors are $\pm 5\%$. c) See Ref. 18. The value at 37 °C. d) See Ref. 14. The value at 20 °C. e) See Ref. 19. The value at 20 °C. Measurement was performed by stopped-flow spectrophotometer. f) See Ref. 31. The value at 25 °C. g) See Ref. 13. The value at 23 °C. h) See Ref. 32. The value for α -tocopheroxyl model radical at 50 °C. i) See Ref. 15. The value at 25 °C.

Table 3. The Values of UV-Visible Absorption Maxima (λ_{\max}^i) and Molar Extinction Coefficients (ε_i) ($i = 1-4$) of the α -, β -, γ -, and δ -Tocopheroxyls and 5,7-Diisopropyltocopheroxyl Radical Model in Ethanol

Toc•	$\lambda_{\max}^1/\text{nm}^{\text{b}}$ ($\varepsilon_1/\text{M}^{-1}\text{cm}^{-1}$)	$\lambda_{\max}^2/\text{nm}^{\text{b}}$ ($\varepsilon_2/\text{M}^{-1}\text{cm}^{-1}$)	$\lambda_{\max}^3/\text{nm}^{\text{b}}$ ($\varepsilon_3/\text{M}^{-1}\text{cm}^{-1}$)	$\lambda_{\max}^4/\text{nm}^{\text{b}}$ ($\varepsilon_4/\text{M}^{-1}\text{cm}^{-1}$)
α -Toc•	428 (4370)	408 (3010)	387sh ^c (1630)	340sh ^c (3790)
β -Toc•	431 (1500) ^d	409 (1200) ^d	—	—
γ -Toc•	432 (820) ^d	—	—	—
δ -Toc•	434 (380) ^d	—	—	—
5,7-Di- <i>i</i> -Pr-Toc• model ^a	420 (4010)	401 (2490)	380sh ^c (1490)	338 (4100)

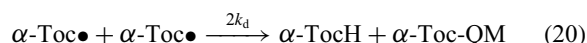
a) See Ref. 37. b) Experimental errors in λ_{\max}^1 , λ_{\max}^2 , and λ_{\max}^3 are ± 1 nm, and in λ_{\max}^4 are ± 5 nm. c) sh: Shoulder. d) The apparent ε_i value (see text).

ethanol shows reasonable agreement with that ($4370 \text{ M}^{-1} \text{ cm}^{-1}$) obtained in the present work.

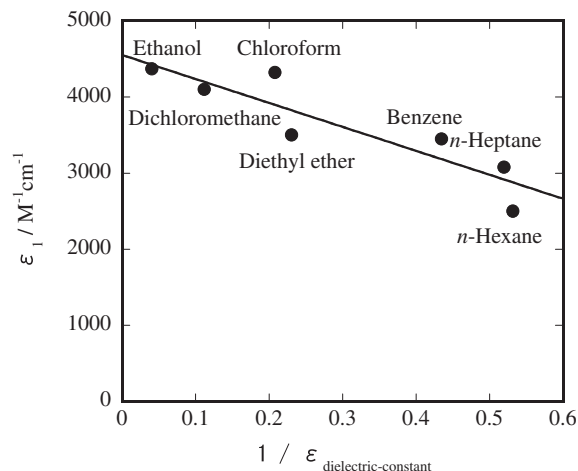
Polarity of the reaction fields of α -TocH in biological systems differs from system to system, and thus measurements were performed in several organic solvents with different polarity, to study the solvent effect on absorption spectra of α -Toc•. As listed in Table 1, the λ_{\max}^1 changes from 418 nm in nonpolar *n*-hexane solvent to 428 nm in polar ethanol solvent. Similar behavior was observed for the λ_{\max}^2 and λ_{\max}^3 . The red shifts of absorption maxima suggest that the transitions are π - π^* .³⁸ The absorption peaks at λ_{\max}^4 are very broad, suggesting the overlap of two absorptions. The relative values of the molar extinction coefficients ($\varepsilon_1:\varepsilon_2:\varepsilon_3:\varepsilon_4$) are similar to each other in these solvents. On the other hand, the values of ε_i ($i = 1-4$) increase with increasing polarity, that is, dielectric constant ($\varepsilon_{\text{dielectric-constant}}$) of the solvents; for instance, the ε_1 value in ethanol is 1.7 times larger than that in *n*-hexane. The ε_1 vs. $1/\varepsilon_{\text{dielectric-constant}}$ plot is shown in Figure 8.

As is clear from the results listed in Table 3, the λ_{\max}^1 values of α -, β -, γ -, and δ -Toc• radicals increase in the order of α - < β - < γ - < δ -Toc• in ethanol. However, the difference in the λ_{\max}^1 values is small, suggesting that the electronic states of these tocopheroxyls are similar to each other. The results of the ESR measurements also indicate that the unpaired electron distributions on α -, β -, γ -, and δ -Toc• radicals are similar to each other in toluene solvent.³⁵ Therefore, we can expect that α -, β -, γ -, and δ -Toc• radicals have similar molar extinction coefficients (ε_i). However, the intensity of the absorption peak of Toc• radicals decreased remarkably in the order of α -Toc• (Absorbance = 0.408 at $\lambda_{\max} = 428$ nm) > β -Toc• (0.131 at 431 nm) > γ -Toc• (0.073 at 432 nm) > δ -Toc• (0.034 at 434 nm) in ethanol, as shown in Figure 6. The reason will be discussed in the following section.

The Rate Constant for the Decay Reaction ($2k_d$) of α -Tocopheroxyl in Organic Solvents. The measurements of the decay rate of α -Toc• radicals in organic solvents have generally been performed by using ESR techniques.^{1,13-19,32} It has been reported that the decay of the α -Toc• follows the bimolecular self-reaction of α -Toc• radicals, suggesting the production of α -TocH and α -tocopherol-*o*-quinonemethide (α -Toc-QM) (Figure 9b) by disproportionation reaction (reaction 20). However, α -Toc-QM is unstable and not isolated.



In the present work, the concentrations (that is, the values of ε) and decay rates ($2k_d$) of α -Toc• were exactly determined in

**Figure 8.** Plot of ε_1 vs. $1/\varepsilon_{\text{dielectric-constant}}$ for α -Toc• radical.

several solvents, using a stopped-flow spectrophotometer and by the simulation of a kinetic model (Figure 4).

The values of $2k_d$ obtained in the present work are summarized in Table 2, together with those reported. The $2k_d$ value ($1.30 \times 10^3 \text{ M}^{-1} \text{ s}^{-1}$) obtained in ethanol is similar to that ($1.4 \times 10^3 \text{ M}^{-1} \text{ s}^{-1}$) reported by Richard et al.¹⁴ and 1.3 and 1.2 times larger than those (1.03×10^3 and $1.06 \times 10^3 \text{ M}^{-1} \text{ s}^{-1}$) reported by Watanabe et al.¹⁸ and Gregor et al.,¹⁹ respectively. Similarly, the $2k_d$ value ($9.50 \times 10^2 \text{ M}^{-1} \text{ s}^{-1}$) in benzene is 1.1 times larger than that ($8.8 \times 10^2 \text{ M}^{-1} \text{ s}^{-1}$) reported by Boguth and Niemann³¹ and 1.2, 3.2, and 6.3 times smaller than those (1.1×10^3 , 3×10^3 , and $6.03 \times 10^3 \text{ M}^{-1} \text{ s}^{-1}$) reported by Roginsky and Krasheninnikova,³² Doba et al.,¹³ and Lucarini et al.,¹⁵ respectively. The $2k_d$ value ($3.00 \times 10^4 \text{ M}^{-1} \text{ s}^{-1}$) obtained in chloroform is 160 times larger than that ($1.9 \times 10^2 \text{ M}^{-1} \text{ s}^{-1}$) reported by Boguth and Niemann.³¹ The reason for such a fast decay of α -Toc• in chloroform is not clear at present.

Scheme of the Decay Reaction of α -, β -, γ -, and δ -Tocopheroxyl Radicals in Organic Solvents. Most of the phenoxyl (PhO•) free radicals are unstable, and decay by fast bimolecular reactions with each other. Bimolecular radical decay of PhO• radical involves dimerization (recombination) and disproportionation reactions.³⁹ Dimers of some PhO• are stable in solution and sometimes may be recovered as solids. Most of such dimers, e.g., dimers of 2,6-di-*tert*-butyl-4R- or 2,6-diphenyl-4R-phenoxyl radicals (for instance, R = CH₃ or C₂H₅), have

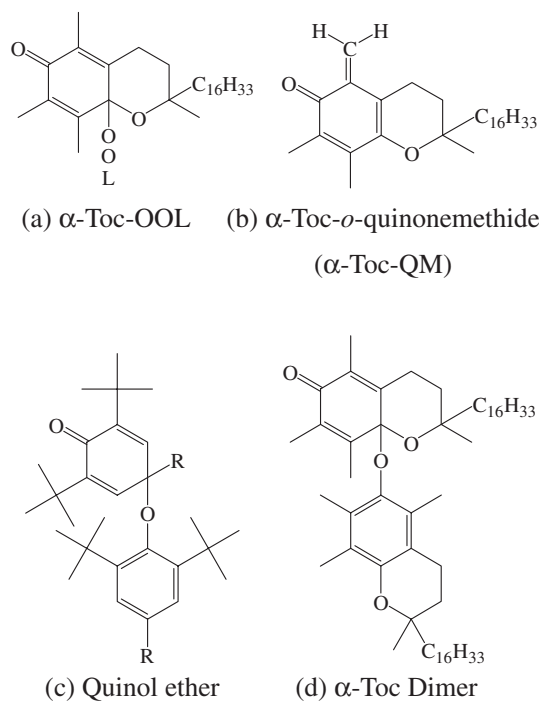
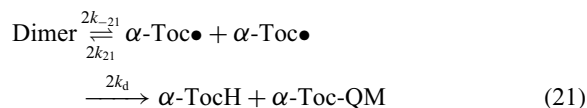


Figure 9. Molecular structures of (a) α -Toc-OOL, (b) α -Toc-*o*-quinonemethide (α -Toc-QM), (c) Quinol ether, and (d) Dimer of α -Toc \bullet radical (α -Toc Dimer).

structures of quinol ethers (“head-to-tail”) (Figure 9c). Structure of the dimer has been ascertained by NMR measurement.⁴⁰ Dimerization reactions of PhO \bullet radicals are fast reactions and are characterized by large rate constants ($k \approx 10^7$ – 10^9 M⁻¹ s⁻¹) in nonviscous solvents at room temperature.

α -Toc \bullet radical in hexane may also decay in two steps as observed for PhO \bullet radicals. First, an equilibrium establishes itself very quickly (with k_{21} and k_{-21}), and then disproportionation reaction 20 with $2k_d$ follows (reaction 21), as proposed by Doba et al.¹³ and ascertained by Lucarini et al.¹⁵ k_{21} and k_{-21} represent the rate constants for the formation and breakdown of dimer, respectively.



where dimer is quinol ether (Figure 9d), although it is unstable and has not been isolated.

Under the condition $k_{21} \gg k_d$, we obtain³⁹

$$-d[\alpha\text{-Toc}\bullet]/dt = k_d[\alpha\text{-Toc}\bullet]^2 / (1 + 2k_{21}[\alpha\text{-Toc}\bullet]/k_{-21}) \quad (22)$$

If $2k_{21}[\alpha\text{-Toc}\bullet]/k_{-21} \gg 1$, radical decay will occur with first-order kinetics and $k_{\text{obsd}} = k_d k_{-21} / 2k_{21}$.

$$-d[\alpha\text{-Toc}\bullet]/dt = (k_d k_{-21} / 2k_{21}) [\alpha\text{-Toc}\bullet] \quad (23)$$

For $2k_{21}[\alpha\text{-Toc}\bullet]/k_{-21} \ll 1$, radical decay will be a second-order reaction with $k_{\text{obsd}} = k_d$.

$$-d[\alpha\text{-Toc}\bullet]/dt = k_d [\alpha\text{-Toc}\bullet]^2 \quad (24)$$

Thus in the case of high concentrations, radicals decay by a first-order reaction, and in the case of low concentrations, by a second-order reaction.

In fact, at low concentration of α -Toc \bullet radical ($t > 5$ s), the decay of α -Toc \bullet radical in hexane may be well explained by a bimolecular disproportionation reaction with a second-order rate constant ($2k_{\text{obsd}} = 2k_d = 1.00 \times 10^3$ M⁻¹ s⁻¹), as shown in Figure 7b. At high concentration of α -Toc \bullet , the decay follows first-order kinetics with $k_{\text{obsd}} = k_d k_{-21} / 2k_{21} = 3.00 \times 10^3$ s⁻¹. Similar analyses were performed for the formation and decay curves observed in diethyl ether and *n*-heptane solvents. The $2k_d$ and k_{-21}/k_{21} values were calculated by assuming the dimerization and disproportionation model shown in reaction 21 and are listed in Table 2.

As described above, the rate constants (k_f) for the formation reaction of α -Toc \bullet radical changed remarkably depending on the polarity of the solvents. The values of k_f ($=k_s$) increased with decreasing polarity of solvent.³³ For example, the values in hexane and benzene are 35 and 19 times larger than those in ethanol, respectively (Table 2). On the other hand, such a solvent dependence was not observed for the rate constants ($2k_d$) of bimolecular reaction. Further, the effect of solvent for $2k_d$ (3.00×10^2 – 1.70×10^3 M⁻¹ s⁻¹) is smaller than that for k_f , except for that in chloroform.

The decay curves of α -Toc \bullet in polar ethanol, dichloromethane, and chloroform solvents were explained by a simple bimolecular reaction without the dimer formation. In fact, the values of ϵ_1 obtained are similar ($\epsilon_1 = 4100$ – 4370 M⁻¹ cm⁻¹) (Table 1). The strong interaction between polar solvent and α -Toc \bullet molecules will hinder the formation of quinol-ether-type dimer in α -Toc \bullet radicals. The nonpolar benzene molecules with an aromatic π -system will also interact with α -Toc \bullet radical molecules that also have an aromatic ring, hindering the formation of dimer. On the other hand, in hexane, heptane, and diethyl ether solvents, α -Toc \bullet radicals are believed to form dimers quickly, and then disappear gradually by bimolecular reaction. The relative ratios of the dimer formation will increase with decreasing polarity of the solvents ($\epsilon_{\text{dielectric-constant}}$), and thus the values of ϵ_1 decrease from $\epsilon_1 = 4370$ M⁻¹ cm⁻¹ in ethanol to 2500 M⁻¹ cm⁻¹ in hexane, as shown in Figure 8 and as listed in Table 1.

Similar measurements were performed for β -, γ -, and δ -TocH, in order to determine the $2k_d$ values for reaction 20. As shown in Figure 6, the same concentration of ArO \bullet radical (8.88×10^{-5} M) was used for the reaction with α -, β -, γ -, and δ -TocH. However, the absorbances of α -, β -, γ -, and δ -Toc \bullet observed decrease rapidly in the order of α -Toc \bullet (Absorbance = 0.408 at $\lambda_{\text{max}} = 428$ nm) > β -Toc \bullet (0.131 at 431 nm) > γ -Toc \bullet (0.073 at 432 nm) > δ -Toc \bullet (0.034 at 434 nm) in ethanol. The smaller absorbance obtained for β -, γ -, and δ -Toc \bullet radicals will be due to the fast formation of dimer (fast equilibrium with the dimer) (reaction 21) in these Toc \bullet radical molecules. In fact, the values of $2k_{21}$ reported for PhO \bullet radicals are very fast and 10^7 – 10^9 M⁻¹ s⁻¹, as described above.³⁹ The steric repulsion due to two *ortho*-methyl groups on α -Toc \bullet radical molecule will hinder the formation of quinol-ether-type dimer. However, the dimer formation will become easier with decreasing the number of *ortho*-methyl groups. As a result, the values of the absorbance decrease in the order of α -Toc \bullet > β -Toc \bullet > γ -Toc \bullet > δ -Toc \bullet radicals in ethanol solvent. In addition to the interaction between solvent and Toc \bullet radical molecules, such steric hindrance will also

have an important effect on the dimer formation. To our regret, we were unsuccessful in determining the ε_i values for β -Toc●, γ -Toc●, and δ -Toc● radicals. However, we may estimate tentatively the apparent ε values ($\varepsilon_{\text{apparent}} = 1500, 820, \text{ and } 380 \text{ M}^{-1} \text{ cm}^{-1}$ (Table 3)) for β -, γ -, and δ -Toc● radicals, respectively, by using the relation (Absorbance (at t_{max}) = $\varepsilon \times [\text{Toc}\bullet] = \varepsilon \times [\text{ArO}\bullet]_{t=0}$). Where the apparent ε values are defined as those for the total molecules which include both i) Toc● monomer and ii) quinol-ether-type Toc● dimer (Figure 9d).

It is well known that the orders of relative tocopherol biopotency using various bioassays⁴¹ and scavenging activities of lipid peroxy¹ and aryloxy^{26,42} radicals by TocH are as follows; α -TocH > β -TocH \geq γ -TocH > δ -TocH. On the other hand, the reverse is the case for the activity to protect fats and oils from oxidation;⁹ α -TocH < β -TocH < γ -TocH < δ -TocH. In general biological systems, such as erythrocyte and mitochondrial membranes, Toc● radicals produced by the reaction with peroxy radicals may be regenerated to TocH by vitamin C^{2,3,10,11} and/or ubiquinol^{3,12,20} (reaction 5), to protect the prooxidant effect (reaction 3). In fats and oils, Toc● radicals react with unsaturated lipids (reaction 3), and induce lipid peroxidation.^{7,9,18} If the Toc● radicals disappear rapidly by the dimer formation and the disproportionation reaction (reaction 21), the prooxidant reaction 3 will be suppressed. This may be one of the reasons why the activity to protect fats and oils from oxidation increases in the order of α -TocH < β -TocH < γ -TocH < δ -TocH.⁹

γ -TocH is the major form of vitamin E in many plant seeds, but has received little attention compared with α -TocH, the predominant form of vitamin E in tissues. However, recently it has been indicated that γ -TocH may be important to human health and that it possesses new attractive functions that distinguish it from α -TocH.⁴³⁻⁴⁵ For example, γ -TocH has higher activity than α -TocH in inhibition of cyclooxygenase activity, and thus γ -TocH suppresses anti-inflammation^{46,47} and inhibits proliferation of prostate cancer cells.⁴⁸ As one of the reasons that γ -TocH shows higher activity than α -TocH, the suppression of the prooxidant effect in γ -TocH may be considered. However, the details are not clear at present.

Conclusion

Kinetic study of the formation and decay reactions of vitamin E radicals (α -, β -, γ -, and δ -tocopheroxyls, Toc●) has been performed in several organic solvents, using stopped-flow spectrophotometry. By mixing α -, β -, γ -, and δ -tocopherols (TocH) with aryloxy radical (ArO●) in organic solvents, the peaks of the UV-vis absorption due to α -, β -, γ -, and δ -Toc● appeared rapidly at 340–430 nm, showed a maximum, and then decayed gradually. We have succeeded in the simulation of the formation and decay curve of α -Toc● radical by the numerical calculation of differential equations related to the above reactions, using the fourth-order Runge–Kutta method. From the results, the second-order rate constants (k_f and $2k_d$) for the formation and decay reactions of α -Toc● and the molar extinction coefficients (ε) of the UV-vis absorption spectra were determined. We can develop this method to more complex reaction systems; for example, the system including ArO●, tocopherol, and ubiquinol-10 (or vitamin C), which is

important in biological systems. The study is now in progress in our laboratory.

We are grateful to Prof. Fernando Antunes of University of Lisbon (Portugal) and Prof. Shin-ichi Nagaoka of Ehime University for their helpful discussions. This work was partly supported by the Grant-in-Aid for Scientific Research on Priority Areas “Applications of Molecular Spins” (Area No. 769, Proposal No. 15087104) from the Ministry of Education, Culture, Sports, Science and Technology (MEXT), Japan (to K. M.).

References

- 1 G. W. Burton, T. Doba, E. Gabe, L. Hughes, F. L. Lee, L. Prasad, K. U. Ingold, *J. Am. Chem. Soc.* **1985**, *107*, 7053.
- 2 E. Niki, *Chem. Phys. Lipids* **1987**, *44*, 227.
- 3 K. Mukai, *Synthesis and Kinetic Study of Antioxidant and Prooxidant Actions of Vitamin E Derivatives in Vitamin E in Health and Disease*, ed. by L. Packer, J. Fuchs, Marcel Dekker, Inc., **1992**, Chap. 8, pp. 97–119.
- 4 L. R. C. Barclay, *Can. J. Chem.* **1993**, *71*, 1.
- 5 J. Cillard, P. Cillard, M. Cormier, L. Girre, *J. Am. Oil Chem. Soc.* **1980**, *57*, 252.
- 6 J. Terao, S. Matsushita, *Lipids* **1986**, *21*, 255.
- 7 S. Nagaoka, Y. Okauchi, S. Urano, U. Nagashima, K. Mukai, *J. Am. Chem. Soc.* **1990**, *112*, 8921.
- 8 V. W. Bowry, R. Stocker, *J. Am. Chem. Soc.* **1993**, *115*, 6029.
- 9 K. Mukai, S. Noborio, S. Nagaoka, *Int. J. Chem. Kinet.* **2005**, *37*, 605.
- 10 J. E. Packer, T. F. Slater, R. L. Willson, *Nature* **1979**, *278*, 737.
- 11 K. Mukai, M. Nishimura, S. Kikuchi, *J. Biol. Chem.* **1991**, *266*, 274.
- 12 *Coenzyme Q: Molecular Mechanisms in Health and Disease*, ed. by V. E. Kagan, P. J. Quinn, CRC Press, **2001**, and references are cited therein.
- 13 T. Doba, G. W. Burton, K. U. Ingold, M. Matsuo, *J. Chem. Soc., Chem. Commun.* **1984**, 461.
- 14 C. Rousseau-Richard, C. Richard, R. Martin, *FEBS Lett.* **1988**, *233*, 307.
- 15 M. Lucarini, G. F. Pedulli, M. Cipollone, *J. Org. Chem.* **1994**, *59*, 5063.
- 16 I. Kohar, M. Baca, C. Suarna, R. Stocker, P. T. Southwell-Keely, *Free Radical Biol. Med.* **1995**, *19*, 197.
- 17 A. Watanabe, N. Noguchi, M. Takahashi, E. Niki, *Chem. Lett.* **1999**, 613.
- 18 A. Watanabe, N. Noguchi, A. Fujisawa, T. Kodama, K. Tamura, O. Cynshi, E. Niki, *J. Am. Chem. Soc.* **2000**, *122*, 5438.
- 19 W. Gregor, G. Grabner, C. Adelwohrer, T. Rosenau, L. Gille, *J. Org. Chem.* **2005**, *70*, 3472.
- 20 K. Mukai, S. Itoh, H. Morimoto, *J. Biol. Chem.* **1992**, *267*, 22277.
- 21 R. H. Bisby, A. W. Parker, *Arch. Biochem. Biophys.* **1995**, *317*, 170.
- 22 S. Nagaoka, T. Kakiuchi, K. Ohara, K. Mukai, *Chem. Phys. Lipids* **2007**, *146*, 26.
- 23 A. A. Remorova, V. A. Roginsky, *Kinet. Catal.* **1991**, *32*, 726.
- 24 K. Mukai, Y. Kohno, K. Ishizu, *Biochem. Biophys. Res. Commun.* **1988**, *155*, 1046.

- 25 S. Nagaoka, K. Sawada, Y. Fukumoto, U. Nagashima, S. Katsumata, K. Mukai, *J. Phys. Chem.* **1992**, *96*, 6663.
- 26 K. Mukai, Y. Watanabe, Y. Uemoto, K. Ishizu, *Bull. Chem. Soc. Jpn.* **1986**, *59*, 3113.
- 27 K. Mukai, K. Daifuku, K. Okabe, T. Tanigaki, K. Inoue, *J. Org. Chem.* **1991**, *56*, 4188.
- 28 S. Nagaoka, A. Kuranaka, H. Tsuboi, U. Nagashima, K. Mukai, *J. Phys. Chem.* **1992**, *96*, 2754.
- 29 W. Cheney, D. Kincaid, *Numerical Mathematics and Computing*, Wadsworth, Belmont, **1985**.
- 30 A. Rieker, K. Scheffler, *Liebigs Ann. Chem.* **1965**, *689*, 78.
- 31 W. Boguth, H. Niemann, *Int. Z. Vitaminforsch.* **1969**, *39*, 429.
- 32 V. A. Roginsky, G. A. Krasheninnikova, *Dokl. Phys. Chem. Acad. Sci. USSR* **1987**, *293*, 263.
- 33 S. Nagaoka, M. Inoue, C. Nishioka, Y. Nishioku, S. Tsunoda, C. Ohguchi, K. Ohara, K. Mukai, U. Nagashima, *J. Phys. Chem. B* **2000**, *104*, 856.
- 34 K. Mukai, N. Tsuzuki, K. Ishizu, S. Ouchi, K. Fukuzawa, *Chem. Phys. Lipids* **1981**, *29*, 129.
- 35 K. Mukai, N. Tsuzuki, S. Ouchi, K. Fukuzawa, *Chem. Phys. Lipids* **1982**, *30*, 337.
- 36 J. Tsuchiya, E. Niki, Y. Kamiya, *Bull. Chem. Soc. Jpn.* **1983**, *56*, 229.
- 37 K. Mukai, Y. Watanabe, K. Ishizu, *Bull. Chem. Soc. Jpn.* **1986**, *59*, 2899.
- 38 H. McConnell, *J. Chem. Phys.* **1952**, *20*, 700.
- 39 E. T. Denisov, I. V. Khudyakov, *Chem. Rev.* **1987**, *87*, 1313.
- 40 D. J. Williams, R. Kreilick, *J. Am. Chem. Soc.* **1968**, *90*, 2775.
- 41 S. Kijima, *Chemistry of Vitamin E in Vitamin E: Its Usefulness in Health and Curing Diseases*, ed. by M. Mino, H. Nakamura, A. T. Diplock, H. J. Kayden, Japan Scientific Societies Press, Tokyo and Karger, Tokyo, **1992**, pp. 3–11.
- 42 K. Mukai, A. Tokunaga, S. Itoh, Y. Kanesaki, K. Ohara, S. Nagaoka, K. Abe, *J. Phys. Chem. B* **2007**, *111*, 652.
- 43 Q. Jiang, S. Christen, M. K. Shigenaga, B. N. Ames, *Am. J. Clin. Nutr.* **2001**, *74*, 714.
- 44 S. W. Leonard, E. Paterson, J. K. Atkinson, R. Ramakrishnan, C. E. Cross, M. G. Traber, *Free Radical Biol. Med.* **2005**, *38*, 857.
- 45 M. G. Traber, J. Atkinson, *Free Radical Biol. Med.* **2007**, *43*, 4.
- 46 Q. Jiang, I. Elson-Schwab, C. Courtemanche, B. N. Ames, *Proc. Natl. Acad. Sci. U.S.A.* **2000**, *97*, 11494.
- 47 Q. Jiang, B. N. Ames, *FASEB J.* **2003**, *17*, 816.
- 48 H.-Y. Huang, A. J. Alberg, E. P. Norkus, S. C. Hoffman, G. W. Comstock, K. J. Helzlsouer, *Am. J. Epidemiol.* **2003**, *157*, 335.